Supporting Information

Friese et al. 10.1073/pnas.0906809106

SI Materials and Methods

Retrograde Tracing and Immunohistochemistry. Analysis of p11–p21 spinal cords was performed on free-floating, 40-μm-thick cryostat sections, and sections from earlier developmental stages were processed on slides. For retrograde tracing of motor neurons, tetramethylrhodamine-labeled dextran (3000MW, Invitrogen) was applied for 3 h to L4 ventral roots of p16 spinal cords using tightly fitting glass capillaries under continued oxygenation. For nerve lesion experiments, the peripheral nerve innervating the quadriceps muscle was cut 3 days before analysis of ATF3 expression. Hindlimb muscles for analysis of muscle spindles and Golgi tendon organs were cut at 20-μm thickness using a cryostat; sections were collected and stained on slides. Acquisition of images was carried out on an Olympus or Zeiss LSM510 Meta confocal microscope.

Anatomical and Statistical Analysis. For statistical analysis of cell size distributions, cell sizes were modeled as a mixture of normal distributions, using the R package "MCLUST" (1, 2). Models with one, two, three, and four mixture components were fitted to the data, for components with equal and unequal variances. For wild-type mice, the optimal model (two components with unequal variances) was chosen based on the Bayesian information criterion. A threshold cell size that optimally separated the two populations was defined as the cell size that minimizes the classification error, given by the area under the population one density greater than the threshold, plus the area under the population two densities less than the threshold, each scaled by the relative proportions of populations one and two obtained in the fitting process (Fig. S1). Images of vGlut1^{on} terminals on ChAT^{on} motor neurons were reconstructed using Neurolucida 8 software. Intensities of Err3 (nuclear) and NeuN (cell body area) immunohistochemistry were determined using ImageJ software (Version 1.42g, National Institutes of Health). Cell size distributions and fluorescent unit intensity frequency histograms were plotted using R software (Version 2.8.1.).

1. Fraley C, Raftery A (2002) Model-based clustering, discriminant analysis, and density estimation. *J Am Stat Assoc* 97:611–631.

2. Fraley C, Raftery A (2006) *MCLUST Version 3 for R: Normal Mixture Modeling and Model-Based Clustering*. Technical Report No. 504 (University of Washington, Seattle).

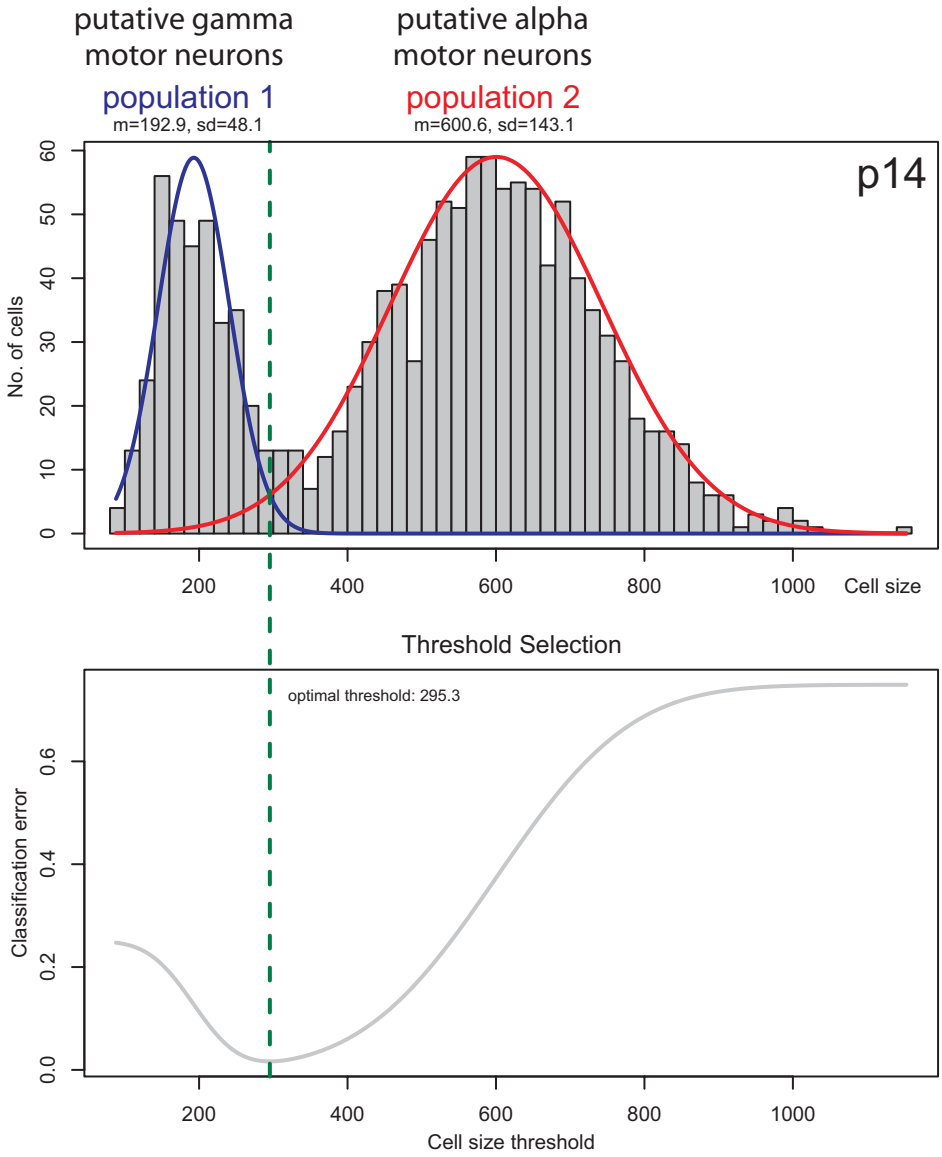

Fig. S1. Quantitative analysis of motor neuron cell size distribution at p14. Cell size distribution of LMC motor neurons in the lumbar spinal cord of p14 wild-type mice. Frequency histogram depicting number of motor neurons in each size bin (*y* axis; binned by 20-μm^2 steps) and size of motor neurons (*x* axis; μm^2). Statistical analysis reveals two normally distributed cell populations (green dotted line: optimal threshold between two populations at 295 μm^2; see *Material and Methods* for details). Bottom graph depicts optimal threshold detection.

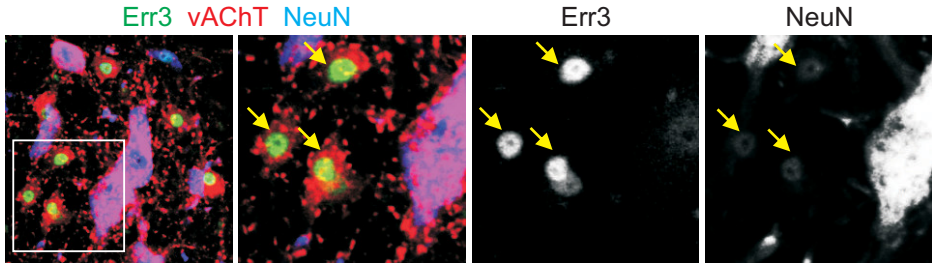

Fig. S2. Putative gamma motor neurons maintain Err^{on} NeuN^{off} status in the adult. Analysis of Err3 and NeuN expression in lumbar motor neurons of 6-week-old wild-type mouse. Analysis of Err3 (green), vAChT (red), and NeuN (blue) in color-combined analysis or by split channels. Box in *left panel* is depicted at higher magnification in *right panels.* Yellow arrows point to putative gamma motor neurons.

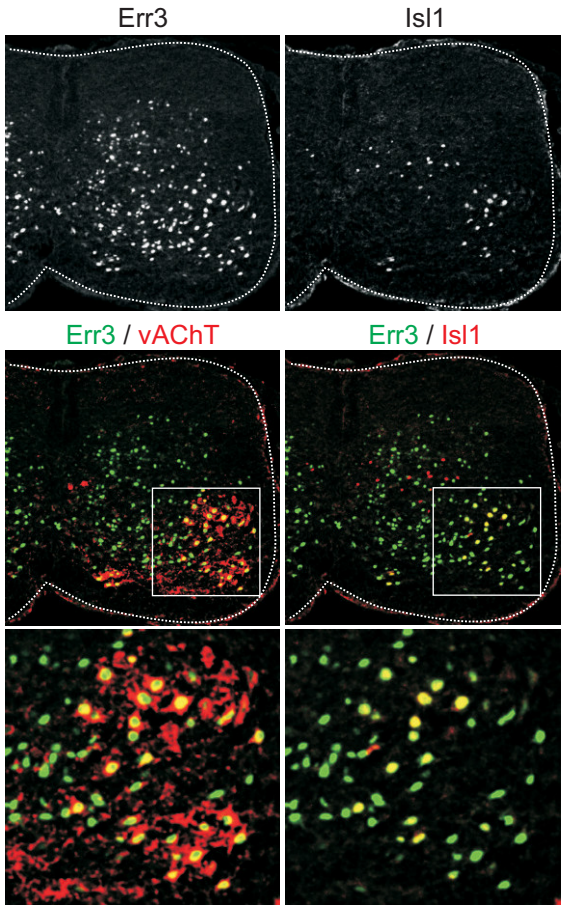

Fig. S3. Widespread expression of Err3 in lumbar motor neurons at p5. Analysis of Err3 expression in lumbar motor neurons of p5 wild-type mouse. Analysis of Err3 (green), vAChT (red; *Left*), and Isl1 (red; *Right*) in color-combined analysis (*Middle*; *Bottom*) or by split channels (*Top*). Boxes in *middle panels* are depicted at higher magnification in *bottom row.* Of note, at p5, many vAChT^{on} motor neurons express Err3, both Isl1^{on} medial LMC as well as Isl1^{off} lateral LMC motor neurons. In contrast, Isl1^{on}/vAChT^{off} dorsal interneurons do not coexpress Err3.

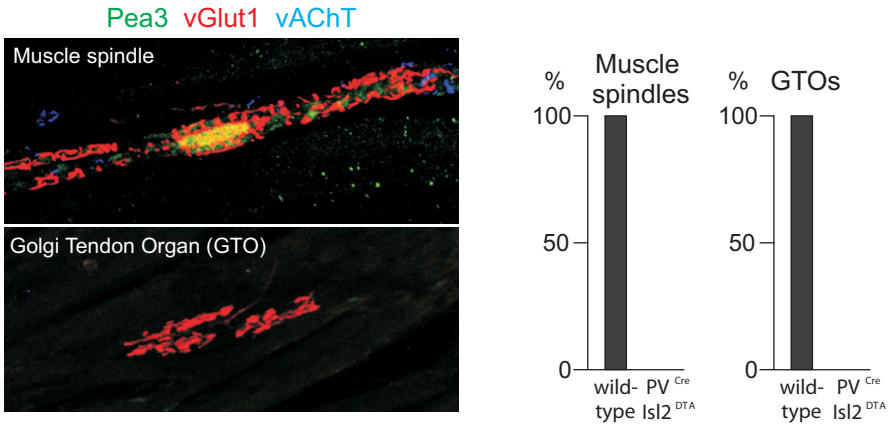

Fig. S4. Muscle spindle and Golgi tendon organ loss in mice lacking proprioceptive afferents. Genetic ablation of proprioceptive afferents in $PV^{Cre}Isl2^{DTA}$ mice leads to absence of muscle spindles and Golgi tendon organ (GTO) in mouse hindlimb muscles. (*Left*) Anatomical identification of muscle spindles (*Top*) and GTOs (*Bottom*) by virtue of Pea3 (green), vGlut1 (red), and vAChT (blue) expression. (*Right*) quantitative analysis reveals complete absence of both muscle spindles and GTOs in p11 $PV^{Cre}Isl2^{DTA}$ mice.